Asociación Argentina
de Mecánica Computacional

Mecánica Computacional Vol XXXVIII, págs. 645-654 (artículo completo)
H.G. Castro, J.L. Mroginski, R.R. Paz, M.A. Storti (Eds.)
Resistencia, 1-5 Noviembre 2021

A TIME-EFFICIENT APPROACH FOR THE COMPUTATIONAL SIMULATION OF CROSS-ROPE TRANSMISSION LINES DYNAMICS UNDER SYNOPTIC WIND LOAD FIELDS

Bruno J. Rango and Marta B. Rosales

Department of Engineering, Universidad Nacional del Sur, Alem 1253, 8000 Bahía Blanca and IFISUR (UNS-CONICET), Argentina, bruno.rango@uns.edu.ar, mrosales@criba.edu.ar

Keywords: Transmission lines, Cross rope tower, stochastic wind load

Abstract. In high and extra-high voltage Overhead Transmission Lines (OTLs), guyed towers are usually preferred over self-supported configurations for economic reasons that derive from their lower weight, which, at the same time, results in a higher slenderness. The structural complexity of these configurations, in addition to the stochastic nature of the main external actions (i.e. wind and ice), has resulted in several academic studies related to the dynamic nonlinear behavior of OTLs. Indeed, the problem has been tackled through analytical, experimental, and computational approaches. Numerical methods, in particular, offer the possibility of implementing parametric sensitivity analyses, which are relevant in this kind of nonlinear dynamic systems. Likewise, through the computational approach, it is possible to derive a robust representation of the structural response by means of the implementation of uncertainty quantification (UQ) studies. However, both types of studies usually require the repeated simulation of the dynamic problem under varying conditions. In such schemes, the dimension of the discretized system can become a limitation. Therefore, it is important to restrict the system number of degrees of freedom, while maintaining a reasonable accuracy in the discretized mathematical model. In this work, a strategy is proposed for the numerical simulation of the dynamic response of an OTL with Cross-Rope supporting structures. The real-life succession of conductor spans and supporting towers is reduced to a single central supporting structure and two adjacent spans. The span continuity of the real system is approximated in this model through the implementation of periodic boundary conditions and linear elastic supports. For the characterization of the boundaries stiffnesses, an optimization scheme based on the Genetic Algorithm is implemented. The resulting system makes it possible to simulate the dynamic response under stochastic synoptic boundary-layer wind load fields within reasonable time in the context of Monte Carlo simulations and parametric sensitivity analyses.

1 INTRODUCTION

Since 2003, Argentina has adopted the Cross-Rope (CR, see Fig. 1) supporting structure configuration for all of the 500 kV Overhead Transmission Lines (OTLs) new projects within the Interconnected National System (Gayo, 2009).

Figure 1: Photograph of an OTL with CR suspension towers.

The action of synoptic boundary layer (SBL) winds on the towers but mainly on the conductor lines constitute the most relevant external load on most of the Argentinian OTLs. Along the literature devoted to the evaluation of transmission lines under the action of wind loads, the problem is tackled through different approaches. in the absence of resources and technical capacities for real-scale field studies or reduced-scale wind tunnel analyses, the numerical framework arises as a valuable tool. In the investigation carried out by Gani and Legeron (2010), for instance, a numerical scheme is adopted for the evaluation of a single-mast guyed suspension tower under SBL wind and ice loads. The succession of towers and spans is reduced by the authors to a single central tower and two adjacent spans of conductor cables. The boundary condition (BC) in the outermost ends of the lines is assumed to be pinned. The same hypotheses were adopted by Rango (2020) and Rango et al. (2019) to model both an OTL with single-mast supporting towers and an OTL with CR supports, under spatially and temporally correlated dynamic wind load fields. The article by Fleck Fadel Miguel et al. (2012) presents a comparison of the outcomes when the IEC 60826 recommended static load model and an spatially correlated stochastic wind load field are applied to an OTL with self-supported towers. Their numerical model consists of four towers and five spans of conductor cables. Likewise, for the evaluation of the dynamic behavior of an OTL with self-supported towers under SBL wind load fields, Yasui et al. (1999) proposed a reduced model composed by three towers and two conductor spans. In summary, the implementation of computational representations of OTLs for the simulation of their dynamic behavior under dynamic wind load fields associated to SBL events, implies the assumption of certain hypotheses, and such hypotheses are diverse along the literature.

The present work is inscribed within a general project devoted to the derivation of a robust representation of the response of OTL systems with guyed supports under the effect of SBL wind events. For this purpose, uncertainty quantification analyses and parametric sensitivity studies are to be performed. However, the implementation of parametric sweeps and UQ studies implies the repeated simulation of the system dynamic response under varying conditions. Thus, these kinds of study result in a high computational demand. Hence, the problem presents a challenging goal: an optimimal model is to be attained, so that its size (measured, for instance, in terms of degrees of freedom (DOFs)) is as small as possible and, at the same time, its capacity to simulate a real-world scenario within acceptable engineering margins is preserved.

In this context, the present investigation is fostered by the hypothesis that it is possible to derive a numerical approach for the simulation of the dynamic response of OTLs with CR supports subjected to the action of SBL winds, which computational demand be suitable for UQ studies and parametric analyses. In this regard, firstly a mathematical model for each of the structural components in the OTL system is stated. The coupled nonlinear system of equations is discretized through the Finite Element Method. On this basis, a nominal and two reduced model are stated. The reference (*i.e.* the nominal) model is conformed by three CR towers and four spans of conductor cables. The number of DOFs in this system is large and definitely not optimal for UQ or parametric analyses. The purpose of this model is to constitute a reference response that allow to compare the outcomes of both reduced models. The first one of these size-reduced models is the same as adopted by Gani and Legeron (2010) and Rango (2020): a central tower and two adjacent spans of conductors in which the outermost ends are assumed as pinned. On the other side, the novel size-reduced model proposed in this work is composed by a central CR suspension tower, two adjacent spans of conductor cables (one span at each side of the tower), and one additional CR tower with elastic supports (instead of guy wires) and periodic BCs at the point of connection between the insulators strings and the outermost ends of the conductors. The stiffnesses of the linear elastic boundaries are tuned by means of an optimization scheme based on the Genetic Algorithm (GA). Once these optimal parameters are determined, the behavior of this model is compared to the target nominal one. The results suggest that the poposed approach provides, in general, better results than the size-reduced model formerly employed by Rango (2020), with very similar computing times.

2 STRUCTURAL MODELS

Model 3T4S: A scheme of the target nominal OTL is represented in Fig. 2. It consists of three CR supporting structures and four conductor spans, therefore it will be identified along this document as Model 3T4S. The dimensions of the structural elements in the CR supports are detailed in Rango (2020). Each CR support is composed of two guyed masts which are connected to each other through the transverse CR cable, from which three insulator chains hung. The conductors are connected to the lower end of the insulator strings. The furthermost ends of the outer conductor spans (with respect to the central CR tower) are assumed to be pinned.

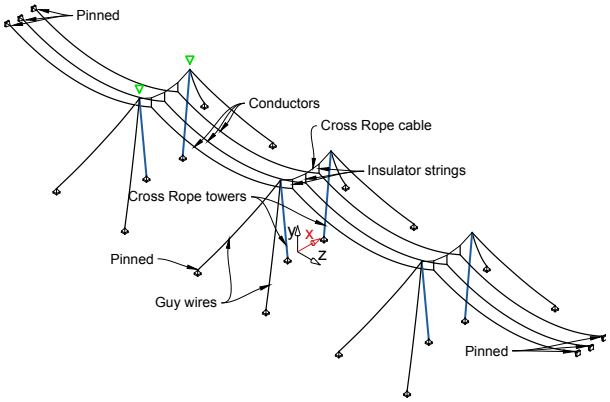

Figure 2: Model 3T4S. Reference configuration composed by three CR supporting structures (CR towers, CR cables and guy wires), 4 spans of conductor cables, and insulator strings. The dimensions along the global x-, y- and z-axis are not represented at the same scale.

Model 1T2S: The structural configuration depicted in Fig. 3a is composed by one central CR support and two adjacent spans of conductor cables with their outermost ends pinned. This configuration has already been reported in the literature (Rango, 2020; Gani and Legeron, 2010), and will be referred along the present document as Model 1T2S.

Model 2T2S: The new structural configuration proposed in this investigation is depicted in Fig. 3b. It consists on a central CR support, two adjacent spans of conductor cables, and a second CR tower. Therefore, the new configuration is identified as Model 2T2S. In order to reduce the number of system DOFs, the geometrically nonlinear guy wires of the second CR tower are replaced by linear translational springs in the global x- and y-directions, placed at the top of the masts. At the same time, the upper end of the masts are assumed to be pinned in the global z-direction. This hypothesis is justified by the fact that the net displacements of the lattices along the global z-direction are negligible, given that the resultant wind load caused by Extended Pressure Systems (such as SBL winds) acting on the whole span of conductor cables is expected to be very similar at both sides of the central tower.

Additionally, with the purpose of simulating the structural continuity of real-life OTLs, periodic BC are defined at the outermost ends of both conductors spans. This is: the displacements along the global x-, y- and z-directions at each pair of structural points indicated with colored dots in Fig. 3b, are assumed to be equal. In this way, the effect of wind on each of the spans of conductors exerts an influence on the other, similarly to real-life structures in which every span is affected by the wind load acting on the adjacent line.

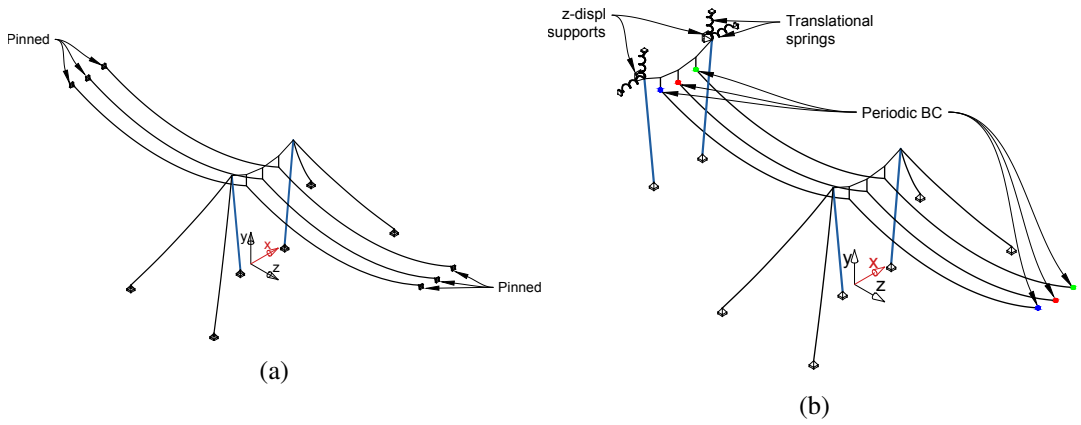

Figure 3: Size-reduced models. (a) Model 1T2S: one central CR support and two spans of conductor cables with pinned conditions in their outermost ends. (b) Model 2T2S: novel configuration conformed by one central CR support, two spans of conductor cables with periodic BC in their outermost ends, and one additional CR tower with linear-elastic supports in the global x- and y- directions instead of guy wires.

3 MATHEMATICAL MODEL

The lattice towers are modeled as unidimensional elastic equivalent beam-columns. The equivalence formulas proposed by Guzmán and Roldan (2021) are adopted to obtain the corresponding mechanical properties. The bending problem in two perpendicular planes which intersect in the longitudinal axis of the beam-column, is formulated according to the Bernoulli-Euler beam theory. At the same time, second order differential equations are associated to the problems of torsional rotations and axial displacements. On the other hand, the conductors, guy

wires, CR, and insulator strings are modeled as elastic unidimensional cables, by means of the geometrically nonlinear formulation proposed by Luongo et al. (1984). This theory is valid for taut cables with sag-to-span ratio lower or equal than 1/10, which happens to be the case for all the cables in this work.

The differential equations that govern the system dynamics as well as the geometric and mechanical properties of the structural elements considered for the present study can be found in Rango (2020). For details on the derivation of those equations, please refer to Ballaben and Rosales (2018).

3.1 Finite Element Discretization

The mathematical system is discretized by means of the Finite Element Method: beam equations are discretized into 2-node linear elements of 12 DOFs (6 at each node) whereas the cable equations are discretized into 3-node curved nonlinear elements of 9 DOFs (3 at each node). The FEM implementation in this work constitute an extension of the FEM software developed by Ballaben (2016) for the nonlinear dynamic analysis of guyed lattice towers. A detailed description of the numerical implementation of the FEM discretization for the present problem, as well as details about the static nonlinear and dynamic solvers, and damping considerations, can be found at Rango (2020).

4 STOCHASTIC WIND MODEL

The action of wind on structures depends on the random total wind speed $\mathcal{V}_T(z,t)$. This stochastic field can be split in two parts: the deterministic mean wind speed $\mu_{\nu_T}(z)$, which varies with the height z above the ground, and the zero-mean turbulent wind part ($\mathcal{V}(z,t)$) which varies not only with height but also in time:

$$\mathcal{V}_T(z,t) = \mu_{\nu_T}(z) + \mathcal{V}(z,t) \tag{1}$$

A typical model for the mean wind speed is defined by the potential profile (IEC 60826). For the characterization of the along-wind turbulent component, the spectrum proposed by Davenport (1961) is adopted. The spatial correlation along the global y- and z-directions (vertical and transverse, respectively) of the turbulent wind field is accounted for through the corresponding cross-spectral function (see Rango (2020)).

In this work, the wind is considered to act both on the conductors and on the CR masts in the global x-direction (see the red axes in Fig. 2, 3a, and 3b). The temporally- and spatially-correlated random wind speed field is simulated as sum of cosines with random frequencies and phase angles by means of the Spectral Representation Method (SRM) (Shinozuka and Jan, 1972).

On this basis, the stochastic wind load field $\mathcal{F}_j(z,t)$ acting on the tower and conductors is computed as:

$$\mathcal{F}_j(z,t) = \frac{1}{2}\rho_a c_d a_w \mu_{v_T}(z)^2 + \rho_a c_d a_w \mu_{v_T}(z)\mathcal{V}_j(z,t). \tag{2}$$

Where c_d is the drag coefficient, ρ_a is the air density and a_w is the area of the element exposed to the wind.

The hypotheses, fundamentals, and details on the wind speed model, as well as on the computational implementation of the SRM to the problem at hand, can be found at Rango (2020).

5 STIFFNESSES OF THE ELASTIC BOUNDARIES

The characteristic stiffnesses of the four springs, namely k_x^W and k_y^W for the elastic supports on the global x- and y-directions on the windward mast, and k_x^L and k_y^L on the leeward mast, must be such that the response of this model to the wind load field, be reasonably similar to the response of Model 3T4S to the same load. Given that the response of the structural system depends on the magnitude of the wind load, the characteristic stiffness of the springs should be defined based on the reference wind speed acting on the structural system. For this purpose, an optimization procedure based on the Genetic Algorithm is proposed.

The Genetic Algorithm is a popular heuristic-stochastic optimization tool inspired by the process of evolution by natural selection. The GA solver starts by generating a random initial population of *individuals*. Each individual is a vector which entries are called *genes*. The genes are realizations of the parameters that are to be optimized in the problem. At each step (called *generation*), the algorithm evaluates the goodness of fit of all the individuals in the population by means of a user-defined objective or *fitness function*. Based upon the outcomes of this evaluation, the algorithm selects a group of individuals called *parents* which will provide their genes to the next generation (*i.e.* the children). The children are generated by three different ways: *elite*, *crossover*, and *mutation*. As the GA evolves, the individuals in each generation gets closer to each other and the solver approaches the optimal solution. When the user-defined stooping criterion is met, the algorithms stops.

For the problem at hand, first, the mean component of the wind load field is applied on Model 3T4S. The static deformed configuration is solved, and the target vector $\bar{\mathbf{u}}$ is recorded. The vector $\bar{\mathbf{u}}$ contains four components, namely: the displacements along the global x- and y-directions at the top of the masts (see the points indicated with inverted green triangles in Fig. 2). Then, the fitness function (Eq. 3) is defined as the Euclidean Norm of the difference between $\bar{\mathbf{u}}$ and the vector $\mathbf{u}(\mathbf{k})$. The vector $\mathbf{u}(\cdot)$ identifies the displacements along the same DOFs, but corresponding to Model 2T2S. Naturally, these displacements are a function of the vector $\mathbf{k}$ of free parameters (*i.e.* the characteristic stiffnesses of the translational springs).

$$f(\mathbf{k}) = \|\bar{\mathbf{u}} - \mathbf{u}(\mathbf{k})\|. \tag{3}$$

This function is finally minimized in Matlab using the built-in implementation of the GA to find the optimal solution for the vector $\mathbf{k}$.

6 RESULTS

In this section, the results of the investigation are reported. Firstly, the outcomes from the optimization of the stiffnesses of the elastic boundaries are presented. Then, the dynamic response of Model 1T2S and Model 2T2S (with optimized elastic BCs) to stochastic SBL wind load fields are compared to the behavior of Model 3T4S. This scheme is repeated for a series of reference wind speeds between 5 and 40 $\mathrm{m/s}$.

6.1 Optimization

For the implementation of the optimization strategy described in Section 5, the Matlab *ga* function is used. The parameters selected for the GA solver are reported in Table 1. For the present problem, it was found that better results and faster convergence was attained if the maximum number of generations was settled to a low number, with a relatively large number of individuals in each generation. An additional stopping criteria was defined through the maximum number of stall generations parameter: it implies that, if after such number of generations

the average relative change in the best fitness value is less than the function tolerance, then the algorithm halts. Regarding the fraction of children that are generated by mutation, elite, and crossover, the default Matlab settings were adopted.

Max. generations	20	Elite individuals	1
Number individuals	200	Crossover fraction	0.8
Max. stall generations	10	Mutation fraction	0.2
Function tolerance	1×10^{-6}		

Table 1: Parameters employed in the GA solver.

The problem is solved for each reference wind speed in the vector $\mathbf{v_0} = [5 : 1 : 40]$ m/s. Given the randomness in the optimization procedure, the GA solver is run five times for each element in $\mathbf{v_0}$, and, the optimial solution $\mathbf{k_{opt}}$ is settled as the mean value. In Fig. 4, the magnitude of the fitness function corresponding to the five optimization tasks are represented as superimposed coloured bars. It can be seen that, for all of the reference wind speeds considered in this work, the best realization of the optimization task (blue bars) leads to a fitness value lower than 0.004 m. Moreover, it can also be obsserved that the worst optimizaiton result (green bars) provides a very acceptable fitness (lower than 0.01 m) as well.

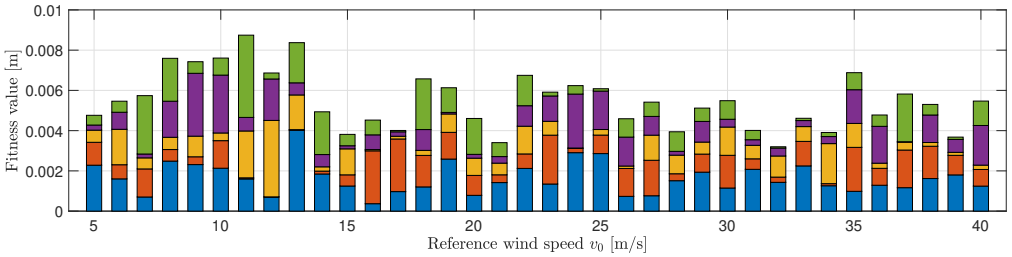

Figure 4: The superimposed coloured bars represent the magnitude of the fitness value associated to the vector of free parameters $\mathbf{k_{opt}}$ in each realization of the optimization task (which is repeated five times) for each reference wind speed considered.

In Fig. 5 the optimal stiffness of the translational springs are reported. It can be observed in Fig. 5a that, as the reference wind speed rises, the stiffness kx^W_{opt} of the spring located at the top of the windward mast in the global x-direction, augments nonlinearly. A parallelism can be drawn between this tendency and the tightening that occurs on the windward guys as the load caused by the action of wind on the structure rises. On the contrary, the leeward guys slackens as the reference wind speed augments, which explains the decay tendency observed in the stiffness kx^L_{opt} of the spring located at the top of the leeward mast in the global x-direction (Fig. 5b). Reasonably, the magnitude of the x-direction elastic supports in the windward mast happens to be appreaciably lower than in the leeward, given that the windward mast experiences higher displacements in that direction than the leeward tower.

The stiffness in the y-direction of the springs in both masts shows a high dispersion (Figs. 5c and 5d) and, a very high magnitude —in general, higher than 1×10^7 N/m—, which suggests that for the range of reference wind speeds considered in this study, the springs in the y-direction behave similarly to a fixed support.

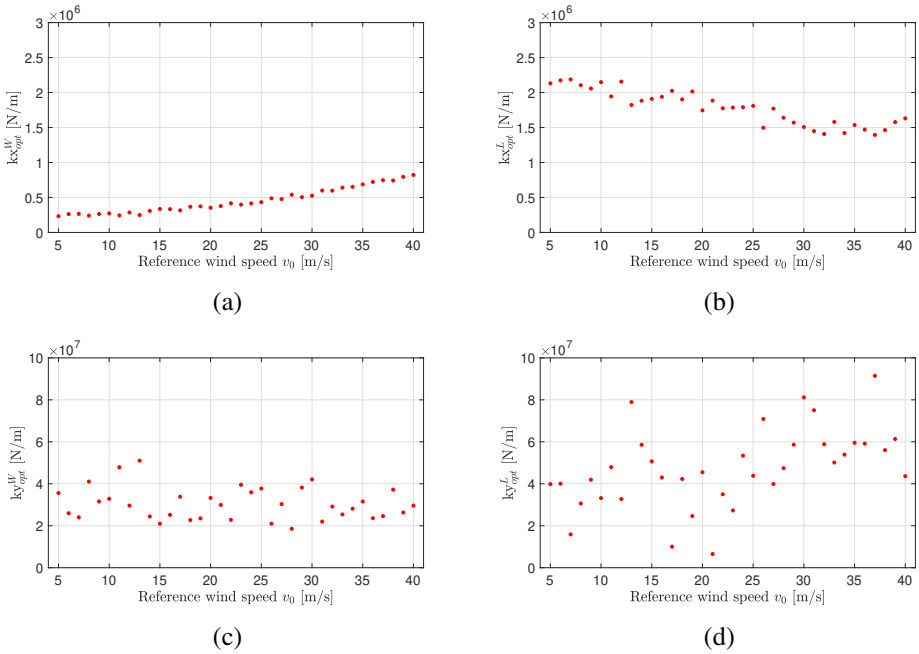

Figure 5: Optimal stiffness of the translational springs: (a) kx^W_{opt}, (b) kx^L_{opt}, (c) ky^W_{opt}, and (d) ky^L_{opt}.

6.2 Comparison of the dynamic responses

In this subsection, the stochastic-dynamic response of the reference Model 3T4S is compared to the behavior of the size-reduced Models 1T2S and 2T2S. For this purpose, a spatially- and temporally-correlated dynamic wind load field is computed and applied to Model 3T4S. The stochastic processes of that field corresponding to nodes in the central CR towers and both adjacent spans of conductor cables are recorded and subsequently applied to Models 1T2S and 2T2S, and the dynamic problem is solved in both of the latter configurations. The average time required for the solution of the dynamic problem was: $t_{3T4S} = 305.21$ minutes for the model 3T4S, $t_{1T2S} = 38.54$ minutes for the Model 1T2S ($t_{1T2S} \approx 0.126 t_{3T4S}$), and $t_{2T2S} = 70.67$ minutes for the Model 1T2S ($t_{1T2S} \approx 0.23 t_{3T4S}$).

The transient response in the global x-direction at the top of the windward mast of the central CR support, is identified as $\mathcal{U}^W_x(t)$. The solid black line in Fig. 6 represents the target stochastic process $\bar{\mathcal{U}}^W_x(t)$, which results from the application to Model 3T4S of a dynamic wind load field characterized by reference speed of 35 m/s. When that same field is applied to Models 1T2S and 2T2S, the process $\mathcal{U}^W_x(t)$ results as indicated by the solid green and red lines of Figs. 6a and 6b, respectively. It can be observed that, for this particular feature of the structural response, and for this reference wind speed, the model 2T2S introduces a visible improvement towards the response of target model.

Finally, in order to compare the results for different magnitudes of the reference wind speed, attention will be focused on the maximum or peak value of certain stochastic processes. For this purpose, the peak values of the stochastic processes obtained from Model 3T4S constitute the nominal response and, on this basis, the relative difference between the latter and the response of Models 1T2S and 2T2S is computed according to: $d_r = (u_{max} - \bar{u}_{max})/\bar{u}_{max}$, where the overline indicates that the magnitude corresponds to the reference Model 3T4S. In Fig. 7a the peak valzes of the displacements along the x-direction at the top of the windward mast ($\mathcal{U}^W_x$), are analyzed. It can be observed that, although both models lead to relative differences of low magnitudes (lower than 0.1), the Model 1T2S underestimates the peak value for

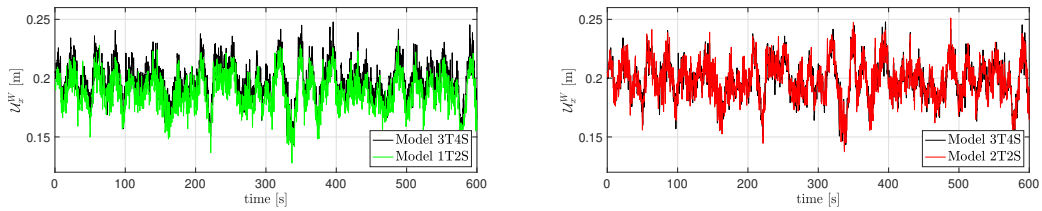

(a) (b)

Figure 6: Comparison of the dynamic response of Model 3T4S, to Models 1T2S and 2T2S.

all the reference wind speeds, whereas Model 2T2S leads to an overestimation of even lower module. For the same stochastic process but in the leeward mast, the behavior is more erratic and both models provide similar relative differences with respect to the Model 3T4S. Figure 7c reports the relative differences in the peak value of the stochastic process $\mathcal{U}_x^C$ associated to the displacements in the x-direction at the center of the windward conductor cable placed on the negative side of the z-coordinates. Again, the figure shows a clear tendency for Model 1T2S to underestimate the target displacements, reaching realtive differences higher than -0.1 for the highest wind speeds. The model 2T2S, on the contrary, leads in general to relative differences of much lower magnitude. Finally, the peak of the stochastic process $\mathcal{H}^{\mathcal{W}}$, associated to the dynamic mechanical tension in one of the windward guys of the central CR support is analyzed in Fig. 7d. The general behavior is repeated: the Model 1T2S underestimates the target and leads, in general, to higher relative differences than the Model 2T2S.

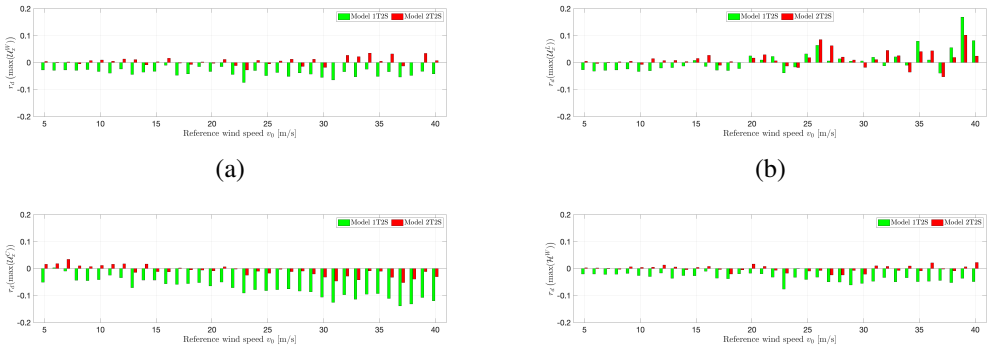

(a) (b)

(c) (d)

Figure 7: Relative difference d_r between the peak values of the stochastic processes of interest .

7 CONCLUSIONS

The purpose of the present investigation was to develop an efficient numerical approach to model an OTL with CR supports. Thus, an approach was proposed and evaluated. The scheme consists in the simplification of the continuous OTL, to a central CR support surrounded by one span of conductor cables at each side, and an additional CR support at the end of one segment. In order to reduce the number of DOFs, the guy wires of the additional CR support were replaced by translational springs along the x- and y-directions, whereas the displacement in the z-direction were restricted. The continuity of towers and spans of conductor cables was simulated through periodic boundary conditions at the end of the lines. A strategy based on Genetic Algorithms was proposed to tune the stiffness of the linear elastic boundaries.

The methodology was successfully implemented. The translational springs were optimized for different magnitudes of the reference wind speed. The extremely high stiffnesses obtained for the springs in the vertical direction indicated that a rigid connection could be assumed in that direction. The optimized parameters were employed for the simulation of the dynamic response of the system under stochastic SBL wind load fields. Moreover, the dynamic response of a second and simpler size-reduced model (Model 1T2S) that has been adopted in previous investigations by the first author, was also simulated. The results from both size-reduced models were compared to the response of reference model of higher size, composed by 3 CR supports and 4 spans of lines. The response of the model proposed in this investigation resulted very similar to that of the target model and, in general, overperformed the outcomes from Model 1T2S. Moreover, even though the new model is slower than Model 1T2S, it allowed a 77% average reduction of the computational simulation time when compared to the reference model.

ACKNOWLEDGMENTS

The authors acknowledge the support given by CONICET, MINCyT, and UNS (Argentina).

REFERENCES

Ballaben J.S. *Mástiles arriostrados: análisis dinámico no lineal y cuantificación de incertidumbres*. Tesis de doctorado, Universidad Nacional del Sur, 2016.

Ballaben J.S. and Rosales M.B. Nonlinear dynamic analysis of a 3d guyed mast. *Nonlinear Dynamics*, 93(3):1395–1405, 2018.

Davenport A. The spectrum of horizontal gustiness near the ground in high winds. *Quarterly Journal of the Royal Meteorological Society*, 87(372):194–211, 1961.

Fleck Fadel Miguel L., Fleck Fadel Miguel L., Riera J., Kaminski J., and Ramos de Menezes J. Assessment of code recommendations through simulation of EPS wind loads along a segment of a transmission line. *Engineering Structures*, 43:1–11, 2012.

Gani F. and Legeron F. Dynamic response of transmission lines guyed towers under wind loading. *Canadian Journal of Civil Engineering*, 37:450–464, 2010.

Gayo R.J. Sistema Interconectado Nacional. *Petrotecnia*, 2009.

Guzmán A.M. and Roldan V.A. Equivalent properties for analysis as beam-column of steel latices of rectangular cross-sectionl. *Advanced Steel Construction*, 2021.

IEC 60826. Design Criteria of Overhead Transmission Lines. International standard, International Electrotechnical Commission (IEC), Geneva, Switzerland, 2003.

Luongo A., Rega G., and Vestroni F. Planar non-linear free vibrations of an elastic cable. *International Journal of Non-Linear Mechanics*, 19(1):39–52, 1984.

Rango B.J. *Dinámica estocástica de cables tensos con aplicaciones a torres arriostradas y líneas de transmisión de energía*. Ph.D. thesis, Universidad Nacional del Sur, 2020.

Rango B.J., Ballaben J.S., Sampaio R., Lima R., and Rosales M.B. Stochastic dynamic response of a cross rope transmission line. In *Mecánica Computacional*, volume 37, pages 679–688. AMCA, 2019.

Shinozuka M. and Jan C. Digital simulation of random processes and its applications. *Journal of Sound and Vibration*, 25(1):111–128, 1972.

Yasui H., Marukawa H., Momomura Y., and Ohkuma T. Analytical study on wind-induced vibration of power transmission towers. *Journal of Wind Engineering and Industrial Aerodynamics*, 83(1-3):431–441, 1999.